Estuarine Exchange Flow Is Related to Mixing through the Salinity Variance Budget

PARKER MACCREADY

University of Washington, Seattle, Washington

W. ROCKWELL GEYER

Woods Hole Oceanographic Institution, Woods Hole, Massachusetts

HANS BURCHARD

Leibniz Institute for Baltic Sea Research, Rostock, Germany

(Manuscript received 15 December 2017, in final form 16 April 2018)

ABSTRACT

The relationship between net mixing and the estuarine exchange flow may be quantified using a salinity variance budget. Here "mixing" is defined as the rate of destruction of volume-integrated salinity variance, and the exchange flow is quantified using the total exchange flow. These concepts are explored using an idealized 3D model estuary. It is shown that in steady state (e.g., averaging over the spring–neap cycle) the volume-integrated mixing is approximately given by Mixing $\cong S_{in}S_{out}Q_r$, where S_{in} and S_{out} are the representative salinities of in- and outflowing layers at the mouth and Q_r is the river volume flux. This relationship provides an extension of the familiar Knudsen relation, in which the exchange flow is diagnosed based on knowledge of these same three quantities, quantitatively linking mixing to the exchange flow.

1. Introduction

An estuary is a bay off the ocean whose circulation and density structure are affected by (i) a source of buoyancy such as a river or net precipitation and (ii) mixing and momentum input due to tides or wind. These conditions give rise to the exchange flow, a persistent inflow of ocean water and outflow of brackish water at the mouth (Hansen and Rattray 1965; MacCready and Geyer 2010), shown schematically in Fig. 1. The exchange flow can be regarded as the volume of water entering the estuary whose salinity is altered by mixing before exiting. Recent research has shown that the physics driving the exchange flow can have surprising complexity (Geyer and MacCready 2014) with the momentum input of tides or wind being important. However, from the earliest analyses (Knudsen 1900; Pritchard 1954; Hansen and Rattray 1965; Chatwin 1976; Walin 1977) onward it has been clear that the creation of mixed water is of central importance. This is most clearly evident in the Knudsen relations (Burchard et al. 2018), and presented in section 2, which demonstrate that the volume flux of the exchange flow may be many times greater than that of the river flow, and this amplification is dependent on the creation of mixed water. While the dependence on mixing is implicit in the Knudsen relations, a direct connection to the rate of mixing by turbulence has been elusive, in part because the word "mixing" may have different definitions in different contexts. The purpose of this paper is to show how a specific definition of mixing, one defined relative to salinity variance, may be linked quantitatively to the exchange flow.

Definitions of mixing

Most commonly, mixing in the oceans (Polzin et al. 1997; Wunsch and Ferrari 2004) and mixing in estuaries (Fischer 1976; Basdurak et al. 2017) is associated with eddy viscosity or diffusivity. However, this mixing measure is not suitable here, since in well-mixed estuaries, when salinity is already fully mixed, salinity mixing vanishes despite high values of eddy diffusivity. Therefore, many estuarine researchers treat mixing in reference to

Denotes content that is immediately available upon publication as open access.

Corresponding author: Parker MacCready, pmacc@uw.edu

DOI: 10.1175/JPO-D-17-0266.1

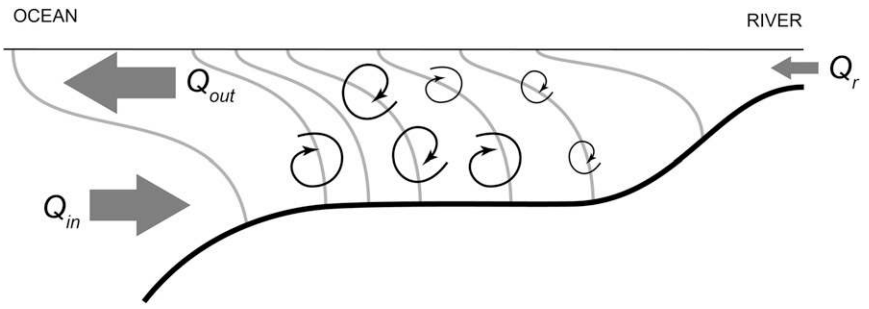

FIG. 1. Sketch of an estuarine along-channel section, indicating isohalines (gray lines), turbulent mixing (curly arrows), and volume transports through the open boundaries. Conceptually the estuary takes in river and ocean waters at rates Q_r and Q_{in}, which are the water-mass end members with high salinity variance. Mixing fills the estuary with a gradation of salinities, all with lower variance, and some part of this mixed water is exported at rate Q_{out}.

the vertical component of Reynolds-averaged turbulent salt flux (Peters and Bokhorst 2001; Li and Zhong 2009). In general, the vertical component of mixing dominates fluxes in geophysical situations because vertical density (or salinity) gradients are typically one or more orders of magnitude greater than horizontal gradients. The turbulent and advective salt fluxes through isohaline surfaces (Walin 1977; MacCready et al. 2002; Wang et al. 2017) have been used as one way to relate the exchange flow to mixing. The fundamental result of this line of inquiry was that the inflow of salt due to the exchange flow must be balanced on average by turbulent and advective salt flux through an isohaline. What has been missing is to connect this back to the Knudsen relations. Wang et al. (2017) explicitly treated mixing using the salinity variance, and the current work builds on that.

Another main tool for the analysis of mixing has been in terms of the buoyancy flux in budgets of potential energy (Simpson et al. 1990; Garvine and Whitney 2006; MacCready et al. 2009; Cessi et al. 2014; Biton and Gildor 2014) or available potential energy (MacCready and Giddings 2016). One disadvantage of this analysis method, as Burchard et al. (2009) point out, is that the sign of the buoyancy flux changes between shear-driven and convectively driven mixing, and it does not represent horizontal mixing processes at all. In addition, the volume-integrated results that relate buoyancy flux to the exchange flow depend on the depth of the interface between inflowing and outflowing branches of the exchange flow at the mouth. In energetic or wide estuarine systems, this depth is difficult to define because of tidal or spatial variability. We find below that these problems are avoided by use of the salinity variance to define mixing.

The dissipation of salinity variance, often designated as χ_s, has long been recognized by the ocean turbulence community as one of the most important quantities representing mixing in the ocean (Nash and Moum 2002; Oakey 1982). In fact for an ocean environment dominated by salinity rather than temperature variance, it is a direct and unambiguous representation of mixing (i.e., the destruction of scalar variance by molecular processes; Tennekes and Lumley 1972). Given the fundamental, unambiguous quality of χ_s as a measure of mixing, it suggests that the salinity variance equation may be the best framework for addressing mixing in environments like estuaries in which density variations are dominated by salinity. Indeed Stern (1968) noted that the input of salinity variance at global scales by evaporation and precipitation has to be balanced on average by the dissipation of salinity variance at molecular scales. A similar balance is obtained in estuaries, but the source of variance derives from the freshwater and ocean inflows.

The most notable recent application of the salinity variance equation with relevance to estuaries is the paper by Burchard and Rennau (2008) in which they use the conservation of salinity variance as a means of quantifying numerically induced mixing in coastal ocean models. More relevant to the results presented here, however, is the application of the salinity variance equation by Burchard et al. (2009) to identify the extreme spatial and temporal variability of mixing in the Baltic Sea. In addition, Wang et al. (2017) use the total exchange flow (TEF) method to relate the exchange flow to volume-integrated mixing in a model of the Hudson River estuary.

2. Equation development

Conservation of salinity s for Reynolds-averaged flow is governed by

$$s_t + \mathbf{u} \cdot \nabla s = \nabla \cdot (K \nabla s), \tag{1}$$

where $\mathbf{u}$ is the 3D velocity vector and K is the eddy diffusivity. The K is treated here as a scalar for mathematical

simplicity, although in our model results there are only vertical turbulent fluxes. Subscript t denotes a time derivative. We assume incompressible flow and zero precipitation and evaporation and denote the volume-averaged salinity as $\bar{s}$, which may in general be a function of time but has no spatial gradients. The salinity variance is then $(s-\bar{s})^2 = s'^2$. Multiplying (1) by $2s'$ we find an equation for the evolution of the variance

$$(s'^2)_t + \mathbf{u}\cdot\nabla(s'^2) = \nabla\cdot(2Ks'\nabla s') - 2K(\nabla s')^2 - 2s'\bar{s}_t. \quad (2)$$

Taking the integral of this over an estuarine volume with open boundaries at the ocean and river ends, and noting that the volume integral of s' is zero, we find the fundamental variance budget:

$$\frac{d}{dt}\int s'^2\,dV = -\int u_n s'^2\,dA_{\text{open}} - 2\int K(\nabla s')^2\,dV, \quad (3)$$

where u_n is the outward-normal velocity on the open boundaries with area A_{open}. Thus, the rate of change of net salinity variance (term on the left) is governed by only two terms: advective inputs of variance at the open boundaries (first term on the right) and loss of variance due to turbulent mixing (second term on the right). The mixing as defined in (3) is positive definite and always acts to destroy variance. Advection may be broken up into three parts: it consists of sources of variance from both the river and the inflowing branch of the exchange flow, while the outflowing branch of the exchange flow removes variance.

The importance of these three advective terms motivates us to use the TEF (MacCready 2011), in which transports through the open boundaries are sorted into salinity classes before tidal averaging and area integration. Here we use the same analysis method for salinity variance. If the flows through the mouth of the estuary were steady and consisted of two layers with uniform properties, then a simple Eulerian average would be sufficient to understand the balance in (3). However, in realistic estuaries the transport is highly variable and there is continuous variation of salinity and variance. In this case the TEF analysis method provides the most robust decomposition of the exchange flow into a compact, two-layer equivalent, creating time series of four tidally averaged variables: Q_{in}, Q_{out}, S_{in}, and S_{out}. These are the tidally averaged transport in and out of the seaward open boundary and the transport-weighted average salinities of these two streams. The same analysis method may be applied to salinity variance instead of salinity (still using salinity as the property for sorting). The volume transport terms are the same, and the resulting transport-weighted average variances will be denoted by S'^2_{in} and S'^2_{out}. We may also perform the analysis on the river-end open boundary (for which salinity = 0). The resulting transport is Q_r, and the transport-weighted salinity variance it carries is $\langle\bar{s}^2\rangle \equiv \overline{S}^2$, where angle brackets denote tidal averaging. The sign convention for the transports is that they are positive when flowing into the estuary volume (Q_{in}, Q_r), whereas Q_{out} is negative. The TEF terms exactly satisfy the time-dependent Knudsen relations (Knudsen 1900; MacCready 2011; Burchard et al. 2018), which are derived from the equation for salt balance in (1) combined with incompressible mass balance, $\nabla\cdot\mathbf{u} = 0$, to find the following:

$$Q_{\text{in}} = \frac{S_{\text{out}}}{\Delta S}Q'_r + \frac{1}{\Delta S}\left\langle\frac{d}{dt}\int s\,dV\right\rangle \quad \text{and}$$
$$-Q_{\text{out}} = \frac{S_{\text{in}}}{\Delta S}Q'_r + \frac{1}{\Delta S}\left\langle\frac{d}{dt}\int s\,dV\right\rangle, \quad (4)$$

where $\Delta S = S_{\text{in}} - S_{\text{out}}$. In deriving (4) we have allowed for changes in tidally averaged estuarine volume by introducing an "adjusted" river flow $Q'_r = Q_r - \langle dV/dt\rangle$. Exact, incompressible, tidally averaged volume conservation is given by $\langle dV/dt\rangle = Q_{\text{in}} + Q_{\text{out}} + Q_r$, or $0 = Q_{\text{in}} + Q_{\text{out}} + Q'_r$. Physically Q'_r is equal in magnitude to the net, tidally averaged volume flux through the mouth of the estuary.

By forming the tidal average of (3) with the advection terms decomposed using the TEF analysis method, we find the tidally averaged variance balance, written in TEF terms:

$$\frac{d}{dt}\left\langle\int s'^2 dV\right\rangle = Q_{\text{in}}S'^2_{\text{in}} + Q_{\text{out}}S'^2_{\text{out}} + Q_r\overline{S}^2 - M. \quad (5)$$

We define tidally averaged net mixing as $M = 2\left\langle\int K(\nabla s')^2\,dV\right\rangle$, a positive-definite quantity that represents the volume-integrated rate of destruction of salinity variance. In most of the remainder of the paper we will refer to this simply as mixing (dropping the "net"), although in a few places mixing will refer to local turbulent processes.

We will use (5) as our primary tool for analyzing the variance budget, but it turns out that we may approximate this budget in a way that yields useful physical insight. If we use the approximation $S'^2_{\text{in}} \approx (S_{\text{in}} - \langle\bar{s}\rangle)^2$, and similar for the "out" terms, then we may combine (4) and (5) to show that (after some manipulation)

$$M \cong S_{\text{in}}S_{\text{out}}Q_r + (S_{\text{in}} + S_{\text{out}} - 2\langle\bar{s}\rangle)\left\langle\frac{d}{dt}\int s\,dV\right\rangle + (\overline{S}^2 - S_{\text{in}}S_{\text{out}})\frac{d\langle V\rangle}{dt} - \left\langle\frac{d}{dt}\int s'^2\,dV\right\rangle. \quad (6)$$

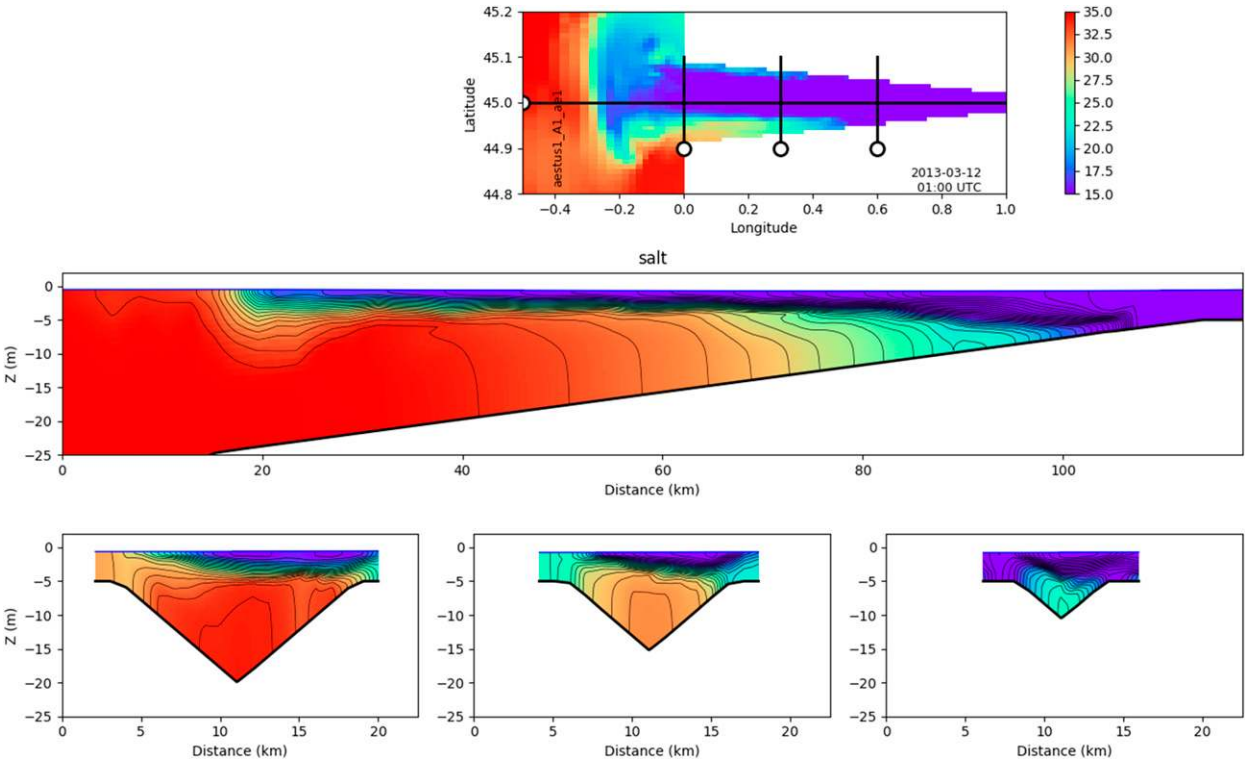

FIG. 2. Model (top) surface salinity and (middle; bottom) sections, during highly stratified, neap tide conditions. (top) The black lines show the locations of the sections, with ''o'' marking the zero distance of the middle and bottom panels. The model domain extends well beyond the limits shown in (top). The dimensions of the whole domain are 315 km by 223 km, and the dimensions of the portion shown are 118 km by 45.5 km. The volume of integration for the analysis goes from the estuary mouth to 1.5° landward. The time of this snapshot corresponds to day 12 of the time series plots.

In steady state, this simplifies to a key result:

$$M \cong S_{\text{in}} S_{\text{out}} Q_r = S_{\text{in}} \Delta S Q_{\text{in}}, \tag{7}$$

which we have written in two different ways using the steady form of the Knudsen relations [(4)]. The final form gives the most succinct answer to the question motivating this study. The exchange flow is quantified as Q_{in}, and S_{in} is close to oceanic salinity. For fixed ΔS this predicts that the exchange flow increases with mixing, but more mixing will also decrease ΔS so there must be a limit to how much mixing can occur. This limit may be inferred from the middle form in (7) as $S_{\text{in}}^2 Q_r$, and we can define a dimensionless measure of ''mixing completeness'' as $\text{Mc} \equiv M/(S_{\text{in}}^2 Q_r)$. Thus, (7) does not completely solve the problem of how much mixing will happen in an estuary, but it gives a very simple way to estimate the average mixing from knowledge of the river flow and typical stratification, in the same way that the Knudsen relations allow estimation of the exchange flow transport. Below we explore the variance budget and its approximation using a numerical model.

3. Model estuary results

We use a numerical simulation of an idealized estuary-shelf system (Figs. 2 and 3) forced with a steady river flow and two tidal constituents that give rise to a spring–neap cycle. This particular configuration was designed to be as simple as possible while still spanning a wide range of estuarine parameter space, from well mixed to strongly stratified on the Geyer and MacCready (2014) parameter space diagram (their Fig. 6). In fact, the parameters that form the axes of that diagram were used to choose the simulation parameters. While this does not give an exhaustive exploration of parameter space (e.g., fjords are neglected), it serves as a useful first test of the use of the variance budget. The simulation is done using the Regional Ocean Modeling System (ROMS; Shchepetkin and McWilliams 2005; Haidvogel et al. 2000), which solves the hydrostatic, incompressible, Reynolds-averaged momentum and tracer conservation equations with a terrain-following vertical coordinate and a free surface. The horizontal domain is a spherical grid extending from longitude −1° to 3° and latitude 44° to 46°N. The grid resolution is 1000 m in the estuary and stretches to 5000 m

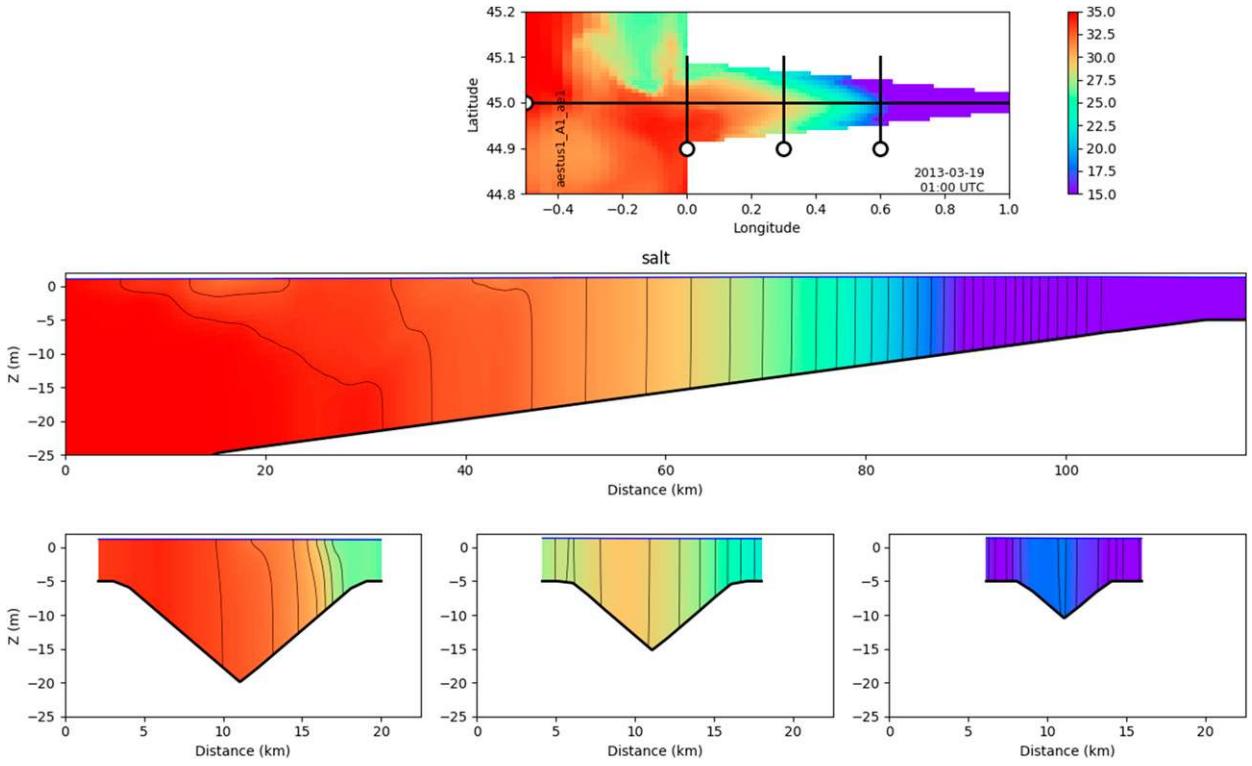

FIG. 3. As in Fig. 2, but during well-mixed, spring tide conditions. The time of this snapshot corresponds to day 19 of the time series plots.

at the boundaries. The model is forced with 1500 $m^3 s^{-1}$ river flow at the eastern end and is initialized with constant salinity of 35 (and zero in the river). Radiation boundary conditions and nudging to initial salinity are used on the open ocean boundaries to maintain the ocean salinity and allow the river plume to exit the domain. The only other forcing is a tidal sea surface height variation on the open boundaries, at M_2 and S_2 frequencies, with amplitudes of 0.75 and 0.25 m, respectively. This gives rise to a pronounced spring–neap cycle. There are 40 vertical layers, and vertical mixing is parameterized using k–ε (turbulent kinetic energy dissipation) with the Canuto-A stability functions (Umlauf and Burchard 2005). Bottom drag followed a quadratic stress law with drag coefficient 3×10^{-3}. The model was run for 3 months with a baroclinic time step of 30 s and had established a nearly repeating spring–neap cycle after the first month. The third month was used for all analysis presented here. Snapshots (history files) were saved hourly, and averages of terms, including salt fluxes, over each hour were also saved. These allowed for construction of budgets with near-perfect conservations of volume and salt, although as we will see salinity variance is still subject to numerical mixing. A 24–24–25 Godin filter (Emery and Thomson 1998) was used for all tidal averaging.

The estuary stratification varies from highly stratified (Fig. 2) to well mixed (Fig. 3) over the spring–neap cycle. The effects of this time variation on the section-integrated transports and stratification are shown in TEF terms in Fig. 4, which covers the third month of the simulation. To form the TEF terms, we start with hourly values of velocity and salinity on a cross section of the estuary, in this case one near the mouth. The volume transport through this section in each model grid cell is binned according to its hourly salinity, in this case using 1000 salinity bins between 0 and 35. The transport in each salinity class is then tidally averaged. From this tidally averaged transport we determine at each time a "dividing salinity" above which the tidally averaged transport is landward and below which the transport is seaward (see appendix). Integrating the transport on either side of this dividing salinity gives us Q_{in} and Q_{out}. We may also form the average salt flux of the in- and outflow streams by integrating the transport times the salinity of each bin on either side of the dividing salinity. Then dividing these by Q_{in} or Q_{out} gives us S_{in} and S_{out}. The same procedure may be generalized to find the flux-weighted average of other quantities, as is done for salinity variance below. The volume-integrated salt budget (Fig. 4a) is dominated by the in- and outflow of the exchange flow. The timing of spring and neap are given by the tidal forcing, expressed as the hourly volume transport through the mouth (Fig. 4b). The volume transports

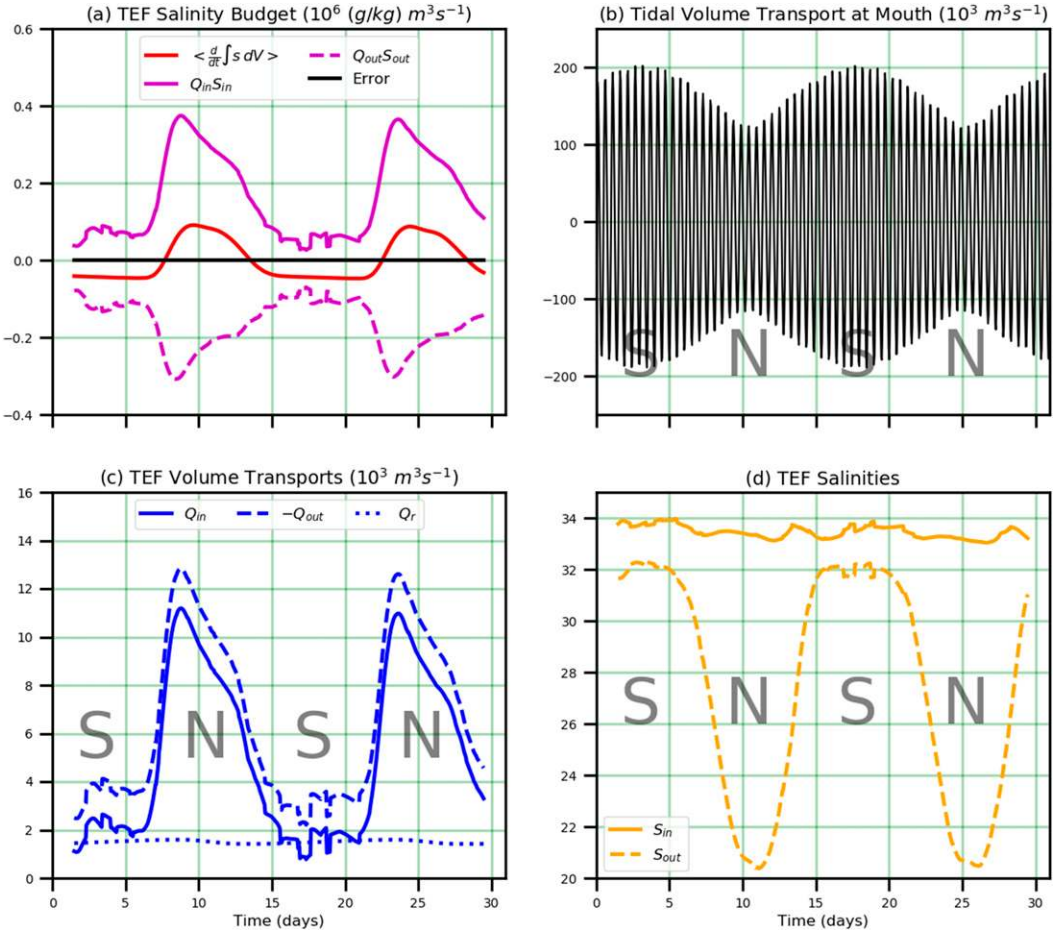

FIG. 4. Terms from the TEF budget. (a) The full, volume-integrated salt budget, and (b) the tidal transport at the mouth, giving the timing of spring and neap forcing. (c) The TEF volume transport terms and (d) the transport-weighted TEF salinities. The small variation of Q_r in (c) is due to subtidal variation of surface height landward of the section where it is calculated. The estuary develops an exchange flow that is many times greater than the river flow. During well-mixed conditions, the exchange flow decreases markedly, and the salinity difference of incoming and outgoing streams becomes small. Times of peak spring and neap tides are marked with "S" and "N" on this and subsequent figures.

(Fig. 4c) show that the exchange flow is amplified by up to 7 times over the river flow, so in this sense the system is clearly acting like an estuary. The stratification at the mouth, quantified as the transport-weighted salinities of the exchange flow, shows strong temporal variation, going from $\Delta S \cong 13$ to 1. The neap-tide restratification and increase in volume-integrated salt are consistent with common understanding. The exchange flow is weak during well-mixed spring tide conditions, and, at that time, the system is losing net salt at a rate close to the river flow times the average salinity.

The time history of the terms in the variance budget [(5)] is shown in Fig. 5a. There is significant time variability of the variance budget, with net rate of increase driven by advection early in neaps and loss driven by mixing at the neap-to-spring transition. Splitting the advection up into its three components (Fig. 5b), the deep inflow of ocean water is the main driver of the early-neap increase, aided by a relatively steady contribution from the river source of freshwater. The outflow at the mouth of brackish water is always a loss term for the net variance. During spring, the exchange of variance at the mouth adds up to almost nothing, and the only source is from the river. The volume-average variance remains relatively steady (Fig. 5c), indicating that much of the variance is contained in the along-channel salinity gradient and not in the vertical stratification.

One useful by-product of the variance budget is that we may use the error, computed as the residual of the budget, as an estimate of the numerical mixing (Burchard and Rennau 2008; Wang et al. 2017) in the model (Fig. 5a). The error arises because the resolved

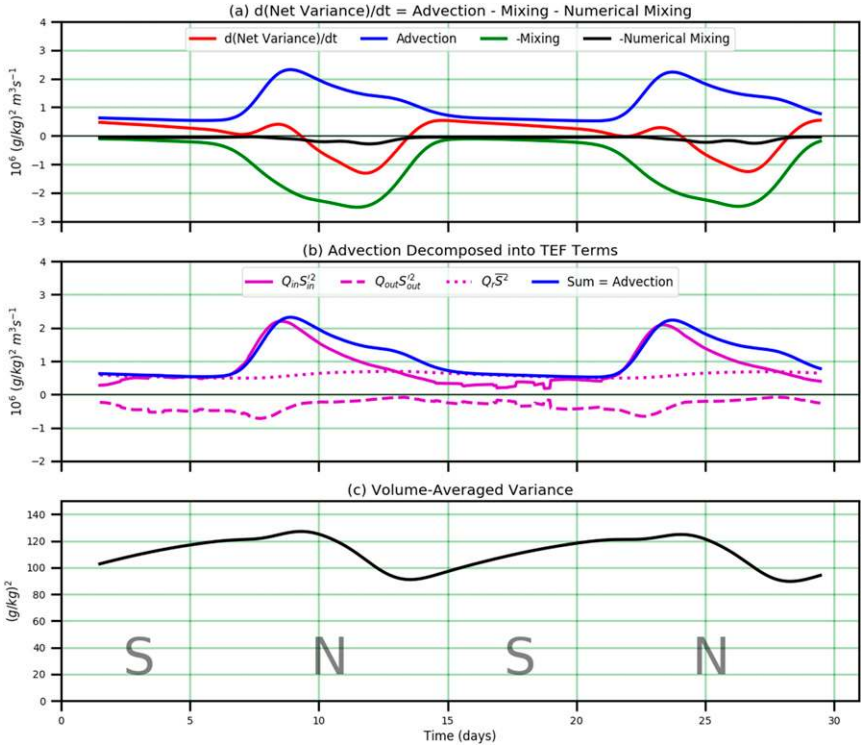

FIG. 5. (a) Terms in the salinity variance budget [(5)], where d(Net Variance)$/dt = d\langle \int s'^2\, dV \rangle /dt$, Advection $= Q_{\text{in}}S_{\text{in}}'^2 + Q_{\text{out}}S_{\text{out}}'^2 + Q_r\overline{S}^2$, and Mixing $= M$. The numerical mixing is whatever additional mixing is required for (5) to close perfectly. The budget is highly time dependent, with mixing happening throughout neap tides and going to near zero during spring tides. (b) The advection is decomposed into TEF terms as given in (5). (c) The volume-average salinity variance $\langle V^{-1} \int s'^2\, dV \rangle$. The river source of variance is rather steady, whereas the exchange flow source and sink are modulated by the tides, becoming smaller in magnitude, and nearly cancelling each other, during springs. These TEF advection terms (magenta) add up to the same blue curve as in (a).

mixing, calculated as $2\left\langle \int K(\partial s/\partial z)^2\, dV \right\rangle$ from hourly snapshots, does not account for all the loss of variance following a fluid particle in the model. Since the tracer advection scheme is not designed to be perfectly variance-conserving there is also numerical mixing. In this case, the numerical mixing is generally small compared to the resolved mixing, but certainly not negligible. Another potential source of error is inaccuracy in the detailed numerics of the budget. However, experiments with the salinity budget (which could be closed with great accuracy) strongly suggest that numerical mixing is the most likely source of error.

Turning to the mixing side of the budget, the resolved mixing and the full mixing (i.e., including numerical mixing) are plotted versus time in Fig. 6a. They have very similar shapes, both peaking at the neap-to-spring transition when strong stratification encounters strong turbulence. As expected, the full mixing is always greater than the resolved mixing. The approximate mixing term in (6) is also plotted and is found to overestimate the peak mixing by about the same amount that the resolved mixing underestimates it. However, the most important result we can get from the approximate budget in (6) is the portion $S_{\text{in}}S_{\text{out}}Q_r$ after averaging over the large spring–neap variation. Averaging over the complete time series using the method described in MacCready (2011), we find $S_{\text{in}} = 33.36$ and $S_{\text{out}} = 25.37$. The estimated average mixing is $S_{\text{in}}S_{\text{out}}Q_r = 1.27 \times 10^6\,(\text{g kg}^{-1})^2\,\text{m}^3\,\text{s}^{-1}$, only about 12% greater than the record-mean full mixing (including numerical mixing), which is $1.13 \times 10^6\,(\text{g kg}^{-1})^2\,\text{m}^3\,\text{s}^{-1}$. This level of error in (7) is surprisingly small given the order-one variation of actual mixing over the spring–neap cycle, suggesting that (7) is a reasonable long-time mean estimate of mixing in estuaries. These mixing values are about 68% of the theoretical maximum $S_{\text{in}}^2Q_r$, that is, a "mixing completeness" of Mc = 0.68. However, we will need to study many more systems to put this percentage in context. Looking more closely into the validity of the approximations used in deriving (6) we see (Fig. 6b) that our TEF approximation of net variance flux is a bit high,

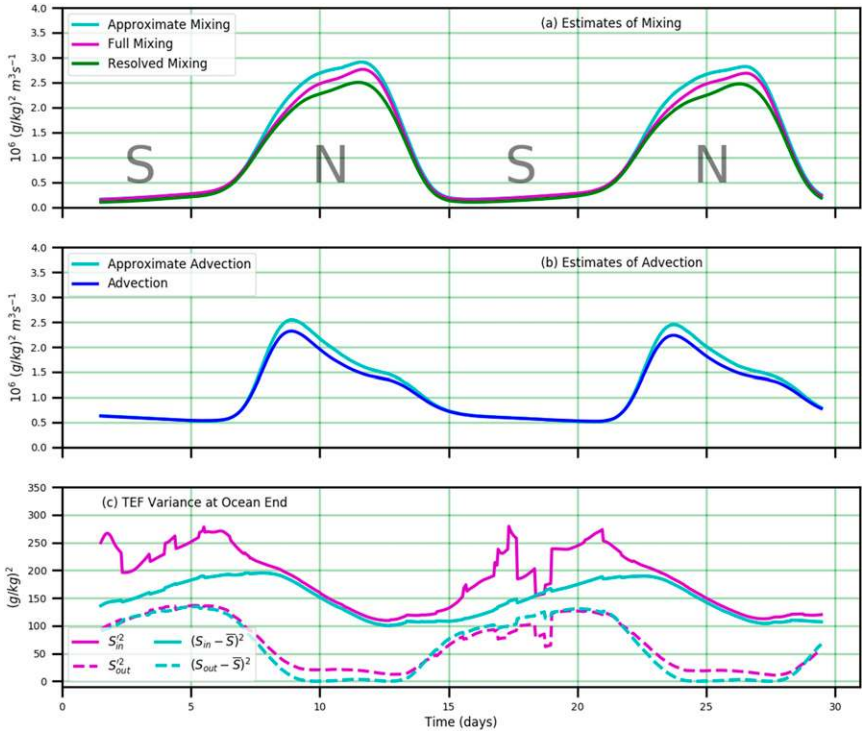

FIG. 6. (a) Three versions of the tidally averaged net mixing. The green "resolved mixing" is M, the negative of the same curve in Fig. 5a. The magenta curve, full mixing, is defined as M + numerical mixing, the mixing based on all other terms in the variance budget. The approximate mixing based on TEF terms (light blue) is equal to the right side of (6). All three estimates are similar, with large spring–neap variation. (b) Two versions of the net advection of variance, where Advection = $Q_{\text{in}}S_{\text{in}}^{\prime 2} + Q_{\text{out}}S_{\text{out}}^{\prime 2} + Q_r\overline{S}^2$, and Approximate Advection = $Q_{\text{in}}(S_{\text{in}} - \langle\overline{s}\rangle)^2 + Q_{\text{out}}(S_{\text{in}} - \langle\overline{s}\rangle)^2 + Q_r\overline{S}^2$. (c) Actual and approximate versions of the TEF in- and outflowing variance at the mouth.

specifically $(S_{\text{out}} - \overline{S})^2 > S^{\prime 2}_{\text{out}}$ during neaps. In addition, the spring–neap cycle is not perfectly periodic, and the storage term contributes about one-fifth of the error. The reason is that our approximation of the outflowing variance is low during highly stratified conditions (Fig. 6c). The errors result from the slight deviation from the assumption of uniform inflow and outflow salinities, not from any conceptual deficiencies of the approach. During unstratified conditions the TEF decomposition of the salinity variance is noisy, but it matters little because the net TEF exchange of variance through the mouth is near zero.

4. Discussion and conclusions

The primary result of this work is the relation in (7), which states that the long-term average mixing in an estuary is approximately given by $S_{\text{in}}S_{\text{out}}Q_r$, or alternatively $S_{\text{in}}\Delta SQ_{\text{in}}$. The significance of this is that it unambiguously relates the mixing to the exchange flow of an estuary. The relationship relies on a specific definition of mixing, one that appears in the variance budget, as opposed to other possible definitions such as the buoyancy flux from the mechanical energy budget. Using an idealized numerical simulation, we have explored this estimate in detail, showing in particular that it only applies to long-term averages. We have limited our exploration to volume integrals of the variance; however, there is potentially much more to be gained in terms of understanding the system function by further decomposition. For example, the full variance can be separated into parts due to horizontal and vertical salinity gradients (Li et al. 2018); to good approximation only the vertical part is subject to mixing.

With respect to the time variability of mixing, this simulation indicates that variance is greatest approaching the neap tide, because of the combination of strong advective input of variance associated with high-salinity inflow and weak mixing. The intensity of mixing increases markedly with increased stratification, even during the weaker turbulence conditions of the neap tide, and the variance drops sharply during this strongly

stratified period. The analysis by Wang et al. (2017) of the dissipation of variance in a realistic model of the Hudson estuary shows a similar phasing of mixing, with the peak occurring several days after the neap tide. Estuaries with stronger or weaker stratification would likely show different phase relationships among the terms in the variance budget.

In terms of consequences to the conditions on the shelf, the salinity of river plumes depends entirely on the amount of mixing that happens in the estuary. This analysis, and especially (7), gives a quantitative way to estimate the amount of mixing that gave rise to any given river plume.

One interesting use of the mixing defined here is that it clearly relates to mixing efficiency (understood as buoyancy flux divided by net turbulence production in a mechanical energy budget). In our simulation, the smallest mixing occurred during springs, when the estuary became vertically well mixed, and in this case, the mixing efficiency has dropped to near zero. This provides an interesting elaboration of the idea of "overmixing" (Stommel and Farmer 1953; Hetland 2010), where the hydraulic control of the exchange flow led to a limit on the amount of mixing that could be supported landward of the control point. In our simulations, as in many estuaries, the regulation of mixing is more dynamic, being strongly modulated in time by the spring–neap cycle. This could be quantified across systems as an added dimension for parameter space diagrams (Geyer and MacCready 2014) in which the net mixing of a system is compared to the maximum possible mixing that the system could support.

Acknowledgments. This research benefited substantially from discussions with Tao Wang and Elizabeth Brasseale. The work was supported by the National Science Foundation through Grants OCE-1736242 to PM and OCE-1736539 to WRG and by the German Research Foundation through Grants TRR 181 and GRK 2000 to HB. The result in (7) was derived independently by WRG and HB.

APPENDIX

Note on the TEF Calculation Method

The well-mixed periods of the spring–neap cycle revealed an important flaw in the standard way of calculating TEF terms. In the usual TEF calculation, the transport is first binned by salinity class and then tidally averaged. Then one calculates Q_{in}, for example, by adding up the transport of all salinity bins for which the transport is positive (MacCready 2011). For reasonably stratified flow, this is relatively insensitive to the number of salinity bins used. However, in well-mixed water the transport in salinity classes can be noisy, and with more salinity bins this noise can result in transport that changes sign many times over the range of salinity classes. When masking by the sign of transport to calculate Q_{in} and Q_{out}, this noise is aliased into increased values of the TEF transports, and the calculated transports grow with increasing numbers of salinity bins. This issue was noted in Lemagie and Lerczak (2015) during times of low stratification. To fix this problem we employ a different method for calculating TEF quantities, one also used in Wang et al. (2017). The strategy is to use the relatively smooth variation of the isohaline transport function, called $Q(s)$ in MacCready (2011, his Fig. 5), which is the integral over salinity of the transport in salinity classes. We integrate from the high-salinity end and then find the salinity at which the transport function is a maximum. Then Q_{in} is the integral of transport in salinity bins above this salinity, and Q_{out} is the integral of transport in fresher salinity bins. The same dividing salinity is used for calculation of the salt flux. Experiments showed that the TEF quantities calculated using this procedure were insensitive to the number of salinity bins over a range from 100 to 1000 (1000 used here).

REFERENCES

Basdurak, N. B., K. D. Huguenard, A. Valle-Levinson, M. Li, and R. J. Chant, 2017: Parameterization of mixing by secondary circulation in estuaries. *J. Geophys. Res. Oceans*, **122**, 5666–5688, https://doi.org/10.1002/2016JC012328.

Biton, E., and H. Gildor, 2014: Energy budget of a small convectively driven marginal sea: The Gulf of Eilat/Aqaba (northern Red Sea). *J. Phys. Oceanogr.*, **44**, 1954–1972, https://doi.org/10.1175/JPO-D-13-0220.1.

Burchard, H., and H. Rennau, 2008: Comparative quantification of physically and numerically induced mixing in ocean models. *Ocean Modell.*, **20**, 293–311, https://doi.org/10.1016/j.ocemod.2007.10.003.

——, F. Janssen, K. Bolding, L. Umlauf, and H. Rennau, 2009: Model simulations of dense bottom currents in the western Baltic Sea. *Cont. Shelf Res.*, **29**, 205–220, https://doi.org/10.1016/j.csr.2007.09.010.

——, and Coauthors, 2018: The Knudsen theorem and the total exchange flow analysis framework applied to the Baltic Sea. *Prog. Oceanogr.*, https://doi.org/10.1016/j.pocean.2018.04.004, in press.

Cessi, P., N. Pinardi, and V. Lyubartsev, 2014: Energetics of semienclosed basins with two-layer flows at the strait. *J. Phys. Oceanogr.*, **44**, 967–979, https://doi.org/10.1175/JPO-D-13-0129.1.

Chatwin, P. C., 1976: Some remarks on the maintenance of the salinity distribution in estuaries. *Estuarine Coastal Mar. Sci.*, **4**, 555–566, https://doi.org/10.1016/0302-3524(76)90030-X.

Emery, W. J., and R. E. Thomson, 1998: *Data Analysis Methods in Physical Oceanography.* Elsevier Science, 634 pp.

Fischer, H. B., 1976: Mixing and dispersion in estuaries. *Annu. Rev. Fluid Mech.*, **8**, 107–133, https://doi.org/10.1146/annurev.fl.08.010176.000543.

Garvine, R. W., and M. M. Whitney, 2006: An estuarine box model of freshwater delivery to the coastal ocean for use in climate models. *J. Mar. Res.*, **64**, 173–194, https://doi.org/10.1357/002224006777606506.

Geyer, W. R., and P. MacCready, 2014: The estuarine circulation. *Annu. Rev. Fluid Mech.*, **46**, 175–197, https://doi.org/10.1146/annurev-fluid-010313-141302.

Haidvogel, D. B., H. G. Arango, K. Hedstrom, A. Beckmann, P. Malanotte-Rizzoli, and A. F. Shchepetkin, 2000: Model evaluation experiments in the North Atlantic basin: Simulations in nonlinear terrain-following coordinates. *Dyn. Atmos. Oceans*, **32**, 239–281, https://doi.org/10.1016/S0377-0265(00)00049-X.

Hansen, D. V., and M. Rattray, 1965: Gravitational circulation in straits and estuaries. *J. Mar. Res.*, **23**, 104–122.

Hetland, R. D., 2010: Estuarine overmixing. *J. Phys. Oceanogr.*, **40**, 199–211, https://doi.org/10.1175/2009JPO4247.1.

Knudsen, M., 1900: Ein hydrographischer Lehrsatz. *Ann. Hydrogr. Marit. Meteor.*, **28**, 316–320.

Lemagie, E. P., and J. A. Lerczak, 2015: A comparison of bulk estuarine turnover timescales to particle tracking timescales using a model of the Yaquina Bay estuary. *Estuaries Coasts*, **38**, 1797–1814, https://doi.org/10.1007/s12237-014-9915-1.

Li, M., and L. Zhong, 2009: Flood–ebb and spring–neap variations of mixing, stratification, and circulation in Chesapeake Bay. *Cont. Shelf Res.*, **29**, 4–14, https://doi.org/10.1016/j.csr.2007.06.012.

Li, X., W. R. Geyer, J. Zhu, and H. Wu, 2018: The transformation of salinity variance: A new approach to quantifying the influence of straining and mixing on estuarine stratification. *J. Phys. Oceanogr.*, **48**, 607–623, https://doi.org/10.1175/JPO-D-17-0189.1.

MacCready, P., 2011: Calculating estuarine exchange flow using isohaline coordinates. *J. Phys. Oceanogr.*, **41**, 1116–1124, https://doi.org/10.1175/2011JPO4517.1.

——, and W. R. Geyer, 2010: Advances in estuarine physics. *Annu. Rev. Mar. Sci.*, **2**, 35–58, https://doi.org/10.1146/annurev-marine-120308-081015.

——, and S. N. Giddings, 2016: The mechanical energy budget of a regional ocean model. *J. Phys. Oceanogr.*, **46**, 2719–2733, https://doi.org/10.1175/JPO-D-16-0086.1.

——, R. D. Hetland, and W. R. Geyer, 2002: Long-term isohaline salt balance in an estuary. *Cont. Shelf Res.*, **22**, 1591–1601, https://doi.org/10.1016/S0278-4343(02)00023-7.

——, N. S. Banas, B. M. Hickey, E. P. Dever, and Y. Liu, 2009: A model study of tide- and wind-induced mixing in the Columbia River estuary and plume. *Cont. Shelf Res.*, **29**, 278–291, https://doi.org/10.1016/j.csr.2008.03.015.

Nash, J. D., and J. N. Moum, 2002: Microstructure estimates of turbulent salinity flux and the dissipation spectrum of salinity. *J. Phys. Oceanogr.*, **32**, 2312–2333, https://doi.org/10.1175/1520-0485(2002)032<2312:MEOTSF>2.0.CO;2.

Oakey, N. S., 1982: Determination of the rate of dissipation of turbulent energy from simultaneous temperature and velocity shear microstructure measurements. *J. Phys. Oceanogr.*, **12**, 256–271, https://doi.org/10.1175/1520-0485(1982)012<0256:DOTROD>2.0.CO;2.

Peters, H., and R. Bokhorst, 2001: Microstructure observations of turbulent mixing in a partially mixed estuary. Part II: Salt flux and stress. *J. Phys. Oceanogr.*, **31**, 1105–1119, https://doi.org/10.1175/1520-0485(2001)031<1105:MOOTMI>2.0.CO;2.

Polzin, K. L., J. M. Toole, J. R. Ledwell, and R. W. Schmitt, 1997: Spatial variability of turbulent mixing in the abyssal ocean. *Science*, **276**, 93–96, https://doi.org/10.1126/science.276.5309.93.

Pritchard, D. W., 1954: A study of the salt balance in a coastal plain estuary. *J. Mar. Res.*, **13**, 133–142.

Shchepetkin, A. F., and J. C. McWilliams, 2005: The regional oceanic modeling system (ROMS): A split-explicit, free-surface, topography-following-coordinate oceanic model. *Ocean Modell.*, **9**, 347–404, https://doi.org/10.1016/j.ocemod.2004.08.002.

Simpson, J. H., J. Brown, J. Matthews, and G. Allen, 1990: Tidal straining, density currents, and stirring in the control of estuarine stratification. *Estuaries*, **13**, 125, https://doi.org/10.2307/1351581.

Stern, M. E., 1968: *T–S* gradients on the micro-scale. *Deep-Sea Res. Oceanogr. Abstr.*, **15**, 245–250, https://doi.org/10.1016/0011-7471(68)90001-6.

Stommel, H., and H. G. Farmer, 1953: Control of salinity in an estuary by a transition. *J. Mar. Res.*, **12**, 13–19.

Tennekes, H., and J. L. Lumley, 1972: *A First Course in Turbulence.* MIT Press, 320 pp.

Umlauf, L., and H. Burchard, 2005: Second-order turbulence closure models for geophysical boundary layers. A review of recent work. *Cont. Shelf Res.*, **25**, 795–827, https://doi.org/10.1016/j.csr.2004.08.004.

Walin, G., 1977: A theoretical framework for the description of estuaries. *Tellus*, **29**, 128–136, https://doi.org/10.3402/tellusa.v29i2.11337.

Wang, T., W. R. Geyer, and P. MacCready, 2017: Total exchange flow, entrainment, and diffusive salt flux in estuaries. *J. Phys. Oceanogr.*, **47**, 1205–1220, https://doi.org/10.1175/JPO-D-16-0258.1.

Wunsch, C., and R. Ferrari, 2004: Vertical mixing, energy, and the general circulation of the oceans. *Annu. Rev. Fluid Mech.*, **36**, 281–314, https://doi.org/10.1146/annurev.fluid.36.050802.122121.